The role of the chemical composition of monetite on the synthesis and properties of α-tricalcium phosphate

Jo Duncan [a], James F. MacDonald [c], John V. Hanna [c], Yuki Shirosaki [d], Satoshi Hayakawa [d], Akiyoshi Osaka [d], Janet M.S. Skakle [a], Iain R. Gibson [a,b,*]

[a] Department of Chemistry, University of Aberdeen, Meston Walk, Aberdeen AB24 3UE, UK
[b] School of Medical Sciences, Institute of Medical Sciences, University of Aberdeen, Foresterhill, Aberdeen AB25 2ZD, UK
[c] Department of Physics, University of Warwick, Gibbet Hill Road, Coventry CV4 7AL, UK
[d] Graduate School of Natural Science and Technology, Okayama University, 3-1-1 Tsushima, Kita-ku, Okayama 700-8530, Japan

ARTICLE INFO

ABSTRACT

There has been a resurgence of interest in alpha-tricalcium phosphate (α-TCP), with use in cements, polymer composites and in bi- and tri-phasic calcium phosphate bone grafts. The simplest and most established method for preparing α-TCP is the solid state reaction of monetite ($CaHPO_4$) and calcium carbonate at high temperatures, followed by quenching.

In this study, the effect of the chemical composition of reagents used in the synthesis of α-TCP on the local structure of the final product is reported and findings previously reported pertaining to the phase composition and stability are also corroborated. Chemical impurities in the monetite reagents were identified and could be correlated to the calcium phosphate products formed; magnesium impurities favoured the formation of β-TCP, whereas single phase α-TCP was favoured when magnesium levels were low. Monetite synthesised in-house exhibited a high level of chemical purity; when this source was used to produce an α-TCP sample, the α-polymorph could be obtained by both quenching and by cooling to room temperature in the furnace at rates between 1 and 10 °C/min, thereby simplifying the synthesis process. It was only when impurities were minimised that the 12 phosphorus environments in the α-TCP structure could be resolved by ^{31}P nuclear magnetic resonance; samples containing chemical impurity showed differing degrees of line-broadening. Reagent purity should therefore be considered a priority when synthesising/characterising the α-polymorph of TCP.

© 2013 Elsevier B.V. All rights reserved.

1. Introduction

Tricalcium phosphate (TCP) is a calcium phosphate mineral with a Ca/P molar ratio of 1.5 and a chemical formula of $Ca_3(PO_4)_2$ [1]. The two most widely studied forms (crystallographic polymorphs) of TCP are the low temperature form β-TCP and the high temperature form α-TCP; there exists also a very high temperature form known as α′ or γ-TCP [2–4]. Due to the chemical and structural similarities of TCP with that of human bone mineral (which is a non-stoichiometric, carbonated-apatite [5]) it interacts readily with the hard tissues of the human body and is said to be 'bioactive' [6].

The α-polymorph of TCP can be used alone or with other phases to form a mouldable, resorbable cement [6–8]. This means that mixing α-TCP with a liquid phase results in the formation of a hard material

[9] that can be used as a fixation device or a bone defect filler and will eventually be completely replaced by the body's own natural bone. A recent review provides a broad overview of the synthesis and use of α-TCP as a biomaterial [10].

A major challenge with α-TCP is that it is only metastable at room temperature, in that it typically must be rapidly cooled, or quenched, from high temperatures (~1300 °C) to 'lock' the structure in place. If it is cooled slowly, β-TCP becomes the principal phase [11]. The substitution of various ions into the structures of TCP is known to alter the transition (α-β/β-α) temperature, e.g. magnesium has been shown to stabilise β-TCP to higher temperatures [11,12] and silicon has been shown to stabilise α-TCP to lower temperatures [13–16].

Monetite, or dicalcium phosphate anhydrous (DCPA; $CaHPO_4$) is commonly used as a reactant phase for solid-state synthesis of many calcium phosphate minerals used in the bioceramics field [17]. The stoichiometry and chemical purity of the monetite are therefore very important as minute quantities of impurities can lead to other phases forming during the synthesis of α-TCP [18,19]. While the use of α-TCP as a component of bone cements [20–22] and polymer composites [23–26] remains topical, attention to details of the impurity levels of reactants used in these studies is often lacking and the role of these on

synthesis/processing conditions and on the properties of the cement/composite is largely ignored. Here we report the effect of chemical composition of different sources of monetite on the phase composition of α-TCP produced by solid state reaction of monetite and calcium carbonate, and the effect of chemical impurities on the thermal stability of the α-TCP.

2. Materials and methods

2.1. Synthesis/acquisition of monetite

Monetite (sample M-WP1) was prepared in-house using a rapid synthesis aqueous precipitation method using equivalent volumes of $Ca(OH)_2$ (98% assay; VWR, UK) and H_3PO_4 (85% assay; Fisher Scientific, UK) suspensions/solutions at concentrations of 2 moles/litre, resulting in a Ca/P molar ratio of 1.00. Briefly, a calcium hydroxide suspension was prepared by addition of $Ca(OH)_2$ into 500 ml distilled water. This suspension was heated to 70 °C, and continuously stirred whilst an equimolar amount of H_3PO_4 solution (500 ml) was added rapidly; the total volume of acid was added within 1–5 seconds. The precipitate-forming mixture was allowed to be stirred together for around 5 minutes with an immediate washing and filtration step after completion of this stirring period; the precipitate (filter cake) was then dried overnight at 90 °C. Additionally, four different sources of monetite were acquired from various chemical suppliers (Sigma Aldrich − M-SIG; Acros − M-ACR; Merck − M-MER; Alfa Aesar − M-ALF) as listed in Table 1.

2.2. Solid-state synthesis of α-tricalcium phosphate

The synthesis of α-TCP was performed by grinding, together in acetone, monetite (various sources) and calcium carbonate (ACS Reagent, 99.9% purity, 0.004% Mg, LOT 05022dj, Sigma Aldrich, UK) in a 2:1 molar ratio (for 0.1 mole product, 13.6059 g CaHPO₄ was mixed with 5.0045 g CaCO₃ to within ± 0.0005 g) so that the calcium to phosphorus ratio (Ca/P) was 1.50. The mixture was dried at 80 °C to remove the majority of the acetone and then subsequently heated at 1300 °C for 16 hours in platinum crucibles in a muffle furnace (Carbolite, UK), reground and heated again at 1300 °C for another 8–12 hours; samples were then quenched to room temperature in air using a clean brass quenching block that was 10 mm thick and 150 × 240 mm in size. The TCP samples produced from the different monetite sources were named according to Table 1 (TCP-WP1, TCP-SIG, TCP-ACR, TCP-MER, TCP-ALF). Heated products were also subject to cooling regimes of 10, 5 and 1 °C min⁻¹ from 1300 °C to room temperature. Additionally, in order to elucidate the thermal stability of the original products formed, samples were also annealed at 1000 °C for time periods of 3, 5, 6 and 8 hours.

2.3. Characterisation of materials

Samples were analysed by X-ray diffraction (XRD) using a D8 Advance X-ray Diffractometer (Bruker, DE) using Cu K-α radiation, a step size of 0.02° 2θ over the range 20°–40° 2θ for a period of 50 minutes to identify phases. XRD patterns were identified with reference to ICDD card numbers as follows: monetite #09-080, hydroxyapatite

Table 1
List of sources of commercially acquired monetite (CaHPO₄; CAS #7757-93-9, EC #231-826-1) samples.

Supplier	Monetite ID name	Product ID	α-TCP ID name
Acros, USA (97%)	M-ACR	215710010	TCP-ACR
Alfa Aesar, UK (98%)	M-ALF	040232	TCP-ALF
Merck, DE (98–100.5%)	M-MER	1022030500	TCP-MER
Sigma Aldrich, UK (98–105%)	M-SIG	C7263500G	TCP-SIG

#09-432, β-tricalcium phosphate #09-169 and α-tricalcium phosphate #09-348. Collected patterns were normalised so that $I_{max} = 100\%$ of maximum intensity = 100 (arbitrary units). Semi-quantitative phase analysis was performed on X-ray patterns collected on slow-cooled products and products annealed at 1000 °C for set periods of time in order to gain an appreciation of the thermal stability of powders. Analysis was performed using the software package TOPAS Academic (Coelho Software, Australia). The variability in the analysis was established by repeating experiments which maintained the α-TCP sample TCP-ACR at 1000 °C for 3, 5 and 6 hours in triplicate; the largest error in phase composition of this set was used as a standard error for slow-cooled samples. Unit cell parameters of the α-TCP samples TCP-WP1 (single phase) and TCP-ACR (lowest amount of β-TCP impurity phase) were also determined using the TOPAS software, using XRD data collected between 10 and 90° 2θ, with a step size of 0.02° 2θ and a count time of 12 seconds/step. The crystallographic starting model used in refinements was based on the data from Mathew et al. based on a monoclinic unit cell [1].

Chemical composition of the monetite samples was analysed by X-ray fluorescence spectroscopy (XRF) at Ceram Ltd., UK; monetite samples were pre-heated in a muffle furnace (Carbolite, UK) to 900 °C in order to dehydrate and decompose CaHPO₄ to Ca₂P₂O₇ in order to minimise the loss on ignition when samples were formed into lithium borate glasses for analysis.

Thermal decomposition behaviour of samples was investigated using thermogravimetry (TG) using a Stanton-Redcroft STA-780 under flowing nitrogen gas.

Morphologies and local stoichiometries were investigated using scanning electron microscopy (SEM) using an Evo MA10 (Zeiss, DE) equipped with an energy dispersive X-ray (EDX) analyser (Inca, Oxford Instruments, UK). Samples were prepared for SEM/EDX by applying a thin layer of powder onto a double sided sticky graphite label that was adhered to an aluminium stub and coated with carbon using an evaporation method.
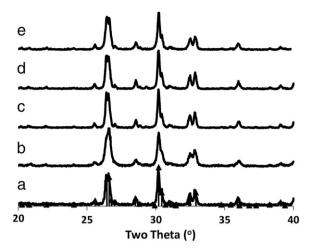
31-Phosphorus magic-angle-spinning nuclear magnetic resonance (³¹P MAS NMR) measurements of all TCP samples were performed at ambient temperatures (~297 K) on a Varian Infinity Plus 300 spectrometer ($B_0 = 7.05$ T) operating at Lamor frequencies of 121.48 MHz (Varian, USA). Single pulse ³¹P experiments were undertaken using a Bruker double-air-bearing 4 mm MAS probe in which MAS frequencies of 12 kHz were achieved using ZrO₂ rotors. A π/4 pulse length of 2 μs and a recycle delay of 300 seconds were used in each measurement, with each acquired experiment consisting of 4 transients. All ³¹P chemical shifts were referenced against the IUPAC standard 85% H₃PO₄ (δ 0.0 ppm) via a secondary solid reference NH₄H₂PO₄ (δ 0.9 ppm). The DMfit software package was used for all deconvolution and simulation of the experimental NMR data [27].

3. Results and discussion

3.1. Characterisation of monetite materials

XRD analysis of the monetite samples indicated that all appeared to be single phase with no impurity phases present (Fig. 1) with the exception of M-ALF (Alfa Aesar) in which diffraction peaks appeared less resolved compared to the other patterns.

The chemical compositions of the different monetite sources used in this study were investigated by analysing their thermally decomposed products (calcium pyrophosphate, Ca₂P₂O₇) by XRF analysis; the data are shown in Table 2. The compositions are reported as oxides in weight-percentage (wt.%) and the limit of detection was 0.02 wt.%. The monetite prepared in-house (M-WP1) had a Ca/P molar ratio of 1.00 (with the error/uncertainty being in the third decimal place) and the amounts of magnesium and silicon present were both less than the limits of detection (<0.02 wt.%). The Ca/P ratios of three of the samples were 0.99–1.00 and the fourth was 0.97 (M-ALF); the magnesium

Fig. 1. X-ray diffraction patterns for samples of monetite (CaHPO₄) used in this study; from bottom to top, the samples were: (a) M-ACR, (b) M-ALF, (c) M-MER, (d) M-SIG and (e) M-WP1. Bragg reflections shown correspond to monetite as detailed in ICDD card number 09-080.
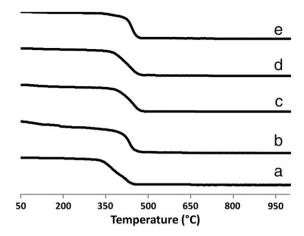

Fig. 2. Normalised thermogravimetric curves showing mass loss events for all samples; from bottom to top, the samples were: (a) M-ACR, (b) M-ALF, (c) M-MER, (d) M-SIG and (e) M-WP1.

oxide contents ranged from 0.11 to 0.99 wt.% (or 0.07 to 0.60 wt.% magnesium) and the silicon oxide contents ranged from 0.13 to 0.59 wt.% (or 0.06 to 0.28 wt.% silicon). Other elements that were measured with values above the limits of detection were aluminium, iron and strontium (0.03 to 0.09 wt.% as oxides). It should be noted that these upper levels of chemical impurities are in the ranges that have been intentionally substituted into calcium phosphates such as hydroxyapatite [28–30] and α-TCP [15] to modify their biological behaviour. Their presence in the reactant phase, and therefore in the synthesised TCP product, is relevant because when implanted, the impurity ions may be released into the surrounding environment.

Due to its "chemical purity," it was hypothesised that synthesis using M-WP1 would yield a single phase stoichiometric α-TCP product as desired with minimal impurities. Conversely, all commercial samples contained impurities to varying degrees and therefore could be less reliable for consistent production of α-TCP; the exception perhaps being the sample M-ACR which showed a total impurity of 0.30% which was the lowest among the commercial samples.

The TG traces for the samples of monetite shown in Fig. 2 demonstrate that the general theme of thermal decomposition of the samples is as expected and is as a result of the mass loss event detailed in Eq. (1) [31,32]:

$$2CaHPO_4 \xrightarrow{\sim 400-500C} \gamma-Ca_2P_2O_7 + \uparrow H_2O \qquad (1)$$

The decomposition event shown in Eq. (1) demonstrates that the theoretical mass loss due to the loss of structural water is 6.62%. M-ALF had both the highest impurity and the largest mass-loss; the remaining four samples showed a mass loss of 7.45% ± 0.10 ($\delta_{6.62\%} = 0.83\% \pm 0.10$) with M-ALF yielding an 8.71% mass-loss. It is

unclear why all samples showed increased levels of mass-loss when compared to the theoretical loss.

SEM images (×10k magnification) of the powder samples of monetite are displayed in Fig. 3a–e. Sample M-WP1 (Fig. 3e) shows the typical morphology expected for monetite (i.e. a rectangular, plate-like crystal [33]). Sample M-ACR (Fig. 3a) was similar but the crystals appeared to have a reduced aspect ratio and consisted of smaller, thicker crystals. Samples M-ALF (Fig. 3b), M-MER (Fig. 3c) and M-SIG (Fig. 3d) showed a similar morphology to one another but different and distinct from the previous samples; these powders showed a general granular morphology with no regular shaped crystalline components observed. The differences in morphologies are likely due to differences in synthesis and/or processing conditions.

SEM in combination with EDX analysis on monetite samples that were found to contain significant magnesium impurities by XRF revealed that the magnesium concentrations were sufficient to be detected in most samples; an example of this is shown in Fig. 4 for sample M-MER. An element map of the same area of the image in 4a is shown in 4b, with a representative composition from a map analysis of this area in 4c. Of the magnesium-containing samples, the sample M-ACR showed the smallest amounts of magnesium by XRF and was not detected by this EDX instrument.

3.2. Characterisation of α-TCP materials

Fig. 5 shows the XRD patterns for all the prepared α-TCP samples; all of these samples were quenched from 1300 °C. The phase compositions of these samples varied significantly and could be related to the chemical compositions of the monetite used (Table 2). The sample TCP-WP1, produced using the monetite synthesised in-house, was single phase α-TCP, whereas the sample TCP-ALF had a biphasic composition consisting of mostly β-TCP with quantities of α-TCP. The monetite used to produce this sample (M-ALF) had the highest level of magnesium impurity (Table 2) and this ion is known to stabilise the β polymorph of TCP [10–12]. The TCP samples produced from the three other commercial monetites were all biphasic compositions with α-TCP as the dominant phase.

The unit cell parameters of the two compositions that produced a single-phase α-TCP product (TCP-WP1) or a near-single phase product (TCP-ACR) were determined from the XRD data and are listed in Table 3. Relative to the parameters of the "chemically pure" TCP-WP1 sample, the major differences in the unit cell parameters of the TCP-ACR sample were an increase in the b-axis and the β angle; these changes are consistent with reported changes in the unit cell of α-TCP with substitution of silicon for phosphorus [15]. TCP-ACR showed more similar levels to

Table 2
Compositions (±0.02%) of pre-heated samples of monetite (CaHPO₄ decomposed to Ca₂P₂O₇) as determined by X-ray fluorescence (XRF). Percentage values less than 0.02% (limit of detection) were omitted for clarity.

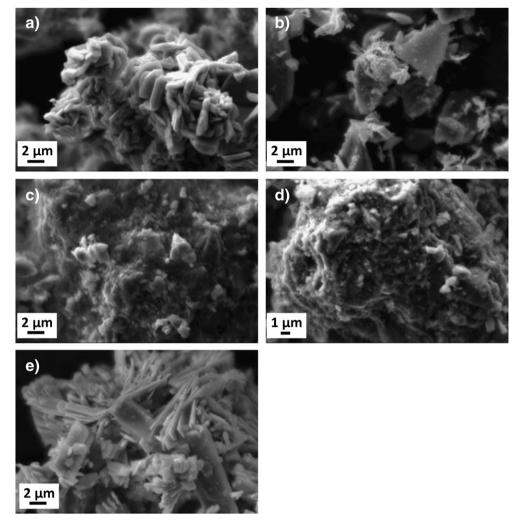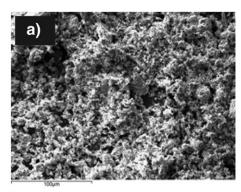| Sample I.D.	Ca/P	CaO (%)	P₂O₅ (%)	MgO (%)	SiO₂ (%)	Al₂O₃ (%)	Fe₂O₃ (%)	SrO (%)
M-WP1	1.00	43.96	55.53	–	–	–	–	–
M-SIG	1.00	43.85	55.60	0.27	0.22	0.04	0.03	–
M-ALF	0.97	42.57	55.69	0.99	0.59	0.09	0.05	0.03
M-MER	1.00	43.93	55.69	0.38	–	–	–	–
M-ACR	0.99	43.85	55.85	0.11	0.13	0.03	–	0.03

Fig. 3. Representative SEM images of monetite samples: (a) M-ACR, (b) M-ALF (c) M-MER, (d) M-SIG and (e) M-WP1.
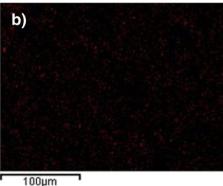
those expected for other axes when comparing to the model proposed by Mathew et al. [1] but when comparing the refined unit cell dimensions with more recent structural refinements on α-TCP [34], TCP-WP1 more closely resembles what was expected.
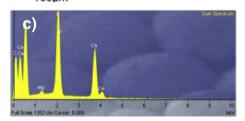
To confirm that further chemical impurities were not introduced into the various TCP compositions from the $CaCO_3$ used in the solid state reaction, sample TCP-WP1 was also analysed by XRF. Results showed that the amount of MgO, SiO_2, Al_2O_3, SrO and Fe_2O_3 impurities were all below the limit of detection (<0.02 wt.%), consistent with the values for the WP1 monetite (Table 2).

^{31}P MAS NMR data of the TCP samples are shown in Fig. 6. A high resolution spectrum showing the full detail of the phosphorus environments in the α-TCP structure was obtained for the TCP-WP1 sample, whereas the other samples produced data of either less defined chemical shifts or, in the case of TCP-ALF, very poorly resolved chemical shifts. The simulation and deconvolution of the data for TCP-WP1 are summarised in Table 4; this revealed that twelve resolved ^{31}P chemical shifts could be fitted to the data. This result corroborates the original X-ray structural solution for α-TCP that proposed twelve chemically independent P positions in the monoclinic unit cell [1]. However, this result conflicts with ^{31}P MAS NMR data reported by Bohner et al. [35] who deconvoluted fifteen ^{31}P resonances from an α-TCP system. It is not clear why such poorly resolved chemical shifts were observed for the TCP samples produced using commercial monetite, but it is likely related to chemical impurities. The sample TCP-ALF (highest magnesium impurity) produced very poorly resolved ^{31}P chemical shifts that relate

well to the ^{31}P MAS NMR chemical shifts of β-TCP [35,36], which is consistent with the XRD data for this sample (Fig. 5).

To test how cooling rate affected the phase compositions obtained, TCP samples were heated to 1300 °C then cooled to room temperature at cooling rates of 1, 5 and 10 °C/min. The resulting percentage of β-TCP formed was determined by Rietveld analysis of the XRD patterns and compared to the values obtained for quenched samples. In Fig. 7a, the data obtained for quenched samples are included and relate to the diffraction patterns in Fig. 5. When samples are cooled from 1300 °C to room temperature at 10 °C/min, the sample TCP-WP1 retained the α-polymorph, whereas all other samples showed an increase in the amount of β-TCP formed compared to quenched samples, although the increase in TCP-ACR was small. Cooling rates of 5 and 1 °C/min resulted in further increases in the amount of β-TCP formed concomitant with magnesium impurity levels. This included sample TCP-WP1 which resulted in a value of 8% β-TCP when a biphasic model was used in the refinement; a single-phase (100% α-TCP) model was also used for the TCP-WP1 pattern but resulted in slightly higher *r*-values. To visualise the correlation between magnesium impurity content and the amount of β-TCP formed in the different samples slow-cooled at 1 °C/min, the amount of β-TCP elucidated was plotted alongside the amount of MgO impurities in the monetite reactant (Fig. 7b), as measured by XRF (Table 2). The importance of MgO impurities in the reactant calcium carbonate on the formation of α-TCP from the solid state reaction with ammonium hydrogen phosphate was noted [37]. Initial studies with a calcium carbonate containing 0.49 wt.% magnesium
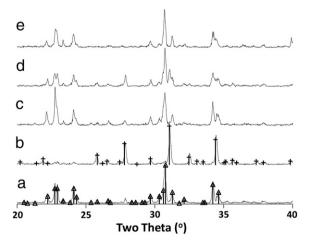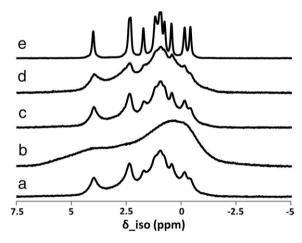
Table 3
Unit cell parameters for α-TCP (TCP-WP1 and TCP-ACR) obtained from Rietveld refinement of X-ray diffraction data; all samples heated at 1300 °C and quenched to room temperature. Data are shown to three decimal places for clarity; errors are rounded estimated standard deviations from TOPAS Academic. Data from literature are included for comparison.

	a (Å)	b (Å)	c (Å)	β (°)
TCP-ACR	12.878(2)	27.309(3)	15.222(2)	126.24(4)
TCP-WP1	12.873(1)	27.262(2)	15.210(1)	126.17(2)
Mathew et al. [1]	12.887(2)	27.280(4)	15.219(2)	126.20(1)
Yashima and Kawaike [34]	12.87271(9)	27.28034(8)	15.21275(12)	126.2078(4)

reported the effect of calcium carbonate purity on the synthesis and hydraulic reactivity of α-TCP [19].

The main finding from the present study is significant as it demonstrates and corroborates that a single phase 100% α-TCP composition can be prepared without the need of a quenching step, using a conventional furnace cooling rate of 10 °C/min when chemically pure reagents are used. It also highlights the negative effect of chemical impurities in the reactants used for α-TCP synthesis on the phase composition. In a review of the studies cited in the present study, most used a solid state synthesis route utilising a quenching step to prepare α-TCP [7,19,21,22,24,37], while the others did not describe the cooling regime used [1,3,23,26] or used a specific cooling rate within the furnace [35]. A recent study noted that it was not possible to produce a single phase α-TCP when using a solid state reaction of calcium carbonate and monetite (both from Sigma Aldrich) [22].

Fig. 4. Elemental analysis of a representative monetite sample; (a) low-magnification SEM image of the sample M-MER (from Merck), (b) magnesium signal (red) from EDX mapping of sample image shown in Fig. 4a, (c) EDX spectrum collected on image shown in Fig. 4a.

impurity (as MgO) resulted in a mixture of α-TCP and β-TCP when quenched from 1300 °C, whereas using a purer calcium carbonate with only 0.01 wt.% Mg resulted in a single phase α-TCP, even between 1125 and 1150 °C. This was recently confirmed by Cicek et al. who
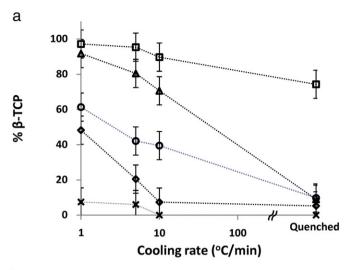

Fig. 6. ^{31}P MAS NMR spectra of quenched TCP samples; from bottom to top the samples were: (a) TCP-ACR, (b) TCP-ALF, (c) TCP-MER, (d) TCP-SIG and (e) TCP-WP1.
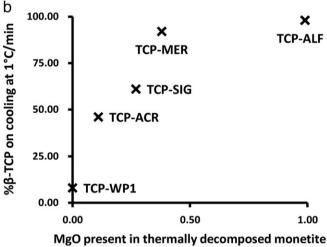

Fig. 5. XRD patterns for samples of quenched TCP samples; from bottom to top the samples were: (a) TCP-ACR, (b) TCP-ALF, (c) TCP-MER, (d) TCP-SIG and (e) TCP-WP1. Solid vertical lines topped with triangles and plus signs show Bragg reflections for α-TCP (ICDD 09-348) and β-TCP (ICDD 09-169), respectively.

Table 4
^{31}P Isotropic chemical shifts (δ_{iso}), FWHM and integrated intensities of "chemically pure" α-TCP (TCP-WP1) using Lorentzian peak shapes.

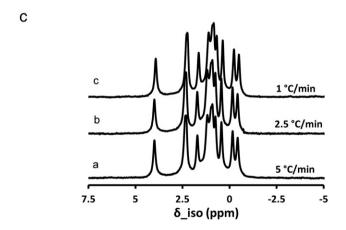| Peak	δ_{iso} (ppm)	FWHM (ppm)	Integrated intensity (%)
1	4.00	0.11	8.07
2	2.38	0.12	8.40
3	2.30	0.11	8.56
4	1.72	0.10	7.77
5	1.19	0.14	10.33
6	1.10	0.20	8.79
7	0.99	0.12	8.28
8	0.91	0.10	7.31
9	0.75	0.10	8.23
10	0.44	0.09	8.00
11	−0.16	0.11	8.47
12	−0.42	0.10	7.79

^{31}P MAS NMR data of the TCP-WP1 samples cooled at different cooling rates (1 and 5 °C/min) were also collected and are shown in Fig. 7c. Similar high resolution chemical shifts were obtained for both cooling rates, comparable to those obtained for the same sample when quenched (Fig. 6), with no appearance of additional shifts that could be related to the formation of β-TCP. The high sensitivity of the NMR data supports the absence of β-TCP in the slow cooled TCP-WP1 samples, and that the small differences in the r-values of the Rietveld refinement between a single- and a biphasic model are not sufficient to support the data fit to the latter.

To further identify the role of chemical purity on the phase stability of the resultant α-TCP phases, the various samples quenched from 1300 °C were then annealed at 1000 °C for various periods of time. The percentage of β-TCP formed was then determined semi-quantitatively by Rietveld analysis of XRD data and were compared to the values obtained for quenched samples (classed as time 0 hour at 1000 °C).

The results in Fig. 8a show similar trends to those in Fig. 7a with the exception of the sample TCP-MER which evolved to produce comparable levels of β-TCP (99%) to that of TCP-ALF (95%) after annealing at 1000 °C for 8 hours. Again, the TCP-WP1 sample showed a small amount of transformation to β-TCP after 3 hours and increased to ~12% after 8 hours of annealing at 1000 °C; all other samples had transformed to >80% β-TCP by this stage. ^{31}P MAS NMR data of the TCP-WP1 samples annealed for 3, 5 and 8 hours at 1000 °C are shown
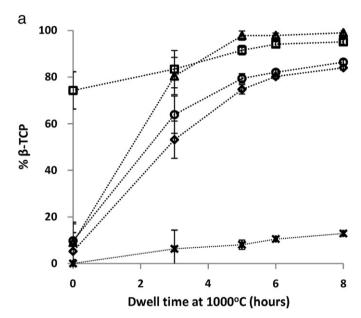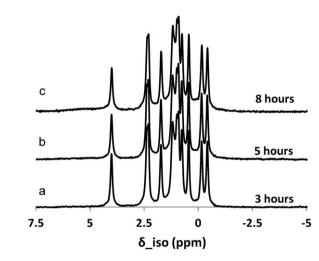

Fig. 7. The effect of cooling rate on the phase composition of TCP samples. (a) Results, expressed as the percentage of β-TCP formed, elucidated by semi-quantitative analysis of XRD patterns of TCP subject to various cooling rates: M-ACR (diamonds), M-ALF (squares), M-MER (triangles), M-SIG (circles), M-WP1 (crosses). Errors represent the largest error elucidated for data in Fig. 8a; (b) the percentage of β-TCP formed from TCP samples cooled at 1 °C/min from 1300 °C related to the MgO impurity content of the corresponding monetite (as pyrophosphate); (c) ^{31}P MAS NMR spectra of TCP-WP1 cooled from 1300 °C to room temperature at 1, 2.5 and 5 °C/min.

Fig. 8. The effect of annealing at 1000 °C on the phase composition of TCP samples. (a) Results, expressed as the percentage of β-TCP formed, elucidated by semi-quantitative analysis of XRD patterns of TCP subject to various lengths of time at 1000 °C: M-ACR (diamonds), M-ALF (squares), M-MER (triangles), M-SIG (circles), M-WP1 (crosses). (b) ^{31}P MAS NMR spectra of TCP-WP1 annealed at 1000 °C for 3, 5 and 8 hours.

in Fig. 8b. Comparable high resolution chemical shifts were obtained for all conditions, with the appearance of a broad shift at ~5.5 ppm related to the formation of β-TCP [35,36].

4. Conclusions

This study showed that the phase composition of calcium phosphate samples with a designed molar ratio of Ca/P = 1.5 is strongly dependent on the chemical purity of the reactant phases; in the case of the current study, the monetite phase. If the reagents used in synthesis are chemically pure then quenching from high temperature becomes unimportant as the α-polymorph is preserved even on slow cooling; it is the presence of impurities (particularly magnesium) that lead to the preference of the formation of β-TCP which necessitates a quenching step to retain the α-polymorph.

The ^{31}P NMR spectra collected showed that the 12 phosphorus environments of the α-TCP structure were only fully realised when an α-TCP product was synthesised using chemically pure reagents.

Acknowledgements

References

[1] M. Mathew, L.W. Schroeder, B. Dickens, W.E. Brown, The crystal structure of α-Ca$_3$(PO$_4$)$_2$, Acta Crystallogr. 33 (1977) 1325–1333.
[2] M. Yashima, A. Sakai, High-temperature neutron powder diffraction study of the structural phase transition between α and α′ phases in tricalcium phosphate Ca$_3$(PO$_4$)$_2$, Chem. Phys. Lett. 372 (2003) 779–783.
[3] A.L. Mackay, A preliminary examination of the structure of α-Ca$_3$(PO$_4$)$_2$, Acta Crystallogr. 6 (1953) 743–744.
[4] M. Descamps, J.C. Hornez, A. Leriche, Effects of powder stoichiometry on the sintering of β-tricalcium phosphate, J. Eur. Ceram. Soc. 27 (2007) 2401–2406.
[5] S. Weiner, W. Traub, Bone structure: from angstroms to microns, FASEB J. 6 (1992) 879–885.
[6] L.L. Hench, Bioceramics, J. Am. Ceram. Soc. 81 (1998) 1705–1727.
[7] X. Wei, O. Ugurlu, M. Akinc, Hydrolysis of α-tricalcium phosphate in simulated body fluid and dehydration behavior during the drying process, J. Am. Ceram. Soc. 90 (2007) 2315–2321.
[8] E. Fernàndez, Bioactive bone cements, in: M. Akay (Ed.), Wiley Encyclopedia of Biomedical Engineering, 6 Volume Set, Wiley, New York, 2006, pp. 1–9.
[9] C. Durucan, P.W. Brown, α-Tricalcium phosphate hydrolysis to hydroxyapatite at and near physiological temperature, J. Mater. Sci. Mater. Med. 11 (2000) 365–371.
[10] R.G. Carrodeguas, S. De Aza, alpha-Tricalcium phosphate: synthesis, properties and biomedical applications, Acta Biomater. 7 (2011) 3536–3546.
[11] G. Berger, R. Gildenhaar, U. Ploska, F.C.M. Driessens, J.A. Plannell, Short-term dissolution behaviour of some calcium phosphate cements and ceramics, J. Mater. Sci. Lett. 16 (1997) 1267–1269.
[12] S. Kannan, J.M. Ventura, J.M.F. Ferreira, Aqueous precipitation method for the formation of Mg-stabilized β-tricalcium phosphate: an X-ray diffraction study, Ceram. Int. 33 (2007) 637–641.
[13] R. Enderle, F. Götz-Neunhoeffer, M. Göbbels, F.A. Müller, P. Greil, Influence of magnesium doping on the phase transformation temperature of β-TCP ceramics examined by Rietveld refinement, Biomaterials 26 (2005) 3379–3384.
[14] M. Kamitakahara, T. Kurauchi, M. Loku, C. Ohtsuki, Synthesis of Si-containing tricalcium phosphate and its sintering behavior, Key Eng. Mater. 361–363 (2008) 59–62.
[15] J.W. Reid, L. Tuck, M. Sayer, K. Fargo, J.A. Hendry, Synthesis and characterization of single-phase silicon-substituted α-tricalcium phosphate, Biomaterials 27 (2006) 2916–2925.
[16] A.M. Pietak, J.W. Reid, M.J. Stott, M. Sayer, Silicon substitution in the calcium phosphate bioceramics, Biomaterials 28 (2007) 4023–4032.
[17] I. Massie, J.M.S. Skakle, I.R. Gibson, Synthesis and phase stability of silicate-substituted alpha-tricalcium phosphate, Key Eng. Mater. 361–363 (2008) 67–70.
[18] J.W. Reid, K. Fargo, J.A. Hendry, M. Sayer, The influence of trace magnesium content on the phase composition of silicon-stabilized calcium phosphate powders, Mater. Lett. 61 (2007) 3851–3854.
[19] G. Cicek, E.A. Aksoy, C. Durucan, N. Hasirci, Alpha-tricalcium phosphate (α-TCP): solid state synthesis from different calcium precursors and the hydraulic reactivity, J. Mater. Sci. Mater. Med. 22 (2011) 809–817.
[20] Y. Qu, Y. Yang, J. Li, Z. Chen, J. Li, K. Tang, Y. Man, Preliminary evaluation of a novel strong/osteoinductive calcium phosphate cement, J. Biomater. Appl. 26 (2011) 311–325.
[21] S.-A. Oh, G.-S. Lee, J.-H. Park, H.-W. Kim, Osteoclastic cell behaviors affected by the a-tricalcium phosphate based bone cements, J. Mater. Sci. Mater. Med. 21 (2010) 3019–3027.
[22] H.-S. Lee, S.Y. Kwon, E.M. Seo, Y.-H. Kim, S.S. Kim, Preparation and characterization of alpha-tricalcium phosphate cements incorporated with polyamino acids, Macromol. Res. 19 (2011) 90–96.
[23] A. Bigi, E. Boanini, G. Maglio, M. Malinconico, R. Palumbo, S.T. Scafati, PLLA based composites with α-tricalcium phosphate and a PLLA-PEO di-block copolymer, Macromol. Symp. 234 (2006) 26–32.
[24] S. Panzavolta, M. Fini, A. Nicoletti, B. Bracci, K. Rubinin, R. Giardino, A. Bigi, Porous composite scaffolds based on gelatin and partially hydrolyzed α-tricalcium phosphate, Acta Biomater. 5 (2009) 636–643.
[25] S.I.J. Wilberforce, C.E. Finlaysone, S.M. Best, R.E. Cameron, A comparative study of the thermal and dynamic mechanical behaviour of quenched and annealed bioresorbable poly-L-lactide/alpha-tricalcium phosphate nanocomposites, Acta Biomater. 7 (2011) 2176–2184.
[26] K. Sakai, Y. Hashimoto, S. Baba, A. Nishiura, N. Matsumoto, Effects on bone regeneration when collagen model polypeptides are combined with various sizes of alpha-tricalcium phosphate particles, Dent. Mater. J. 30 (2011) 913–922.
[27] D. Massiot, F. Fayon, M. Capron, I. King, S. Le Celve, B. Alonson, J.O. Durand, B. Bujoli, Z.H. Gan, G. Hoatson, Modelling one- and two-dimensional solid-state NMR spectra, Magn. Reson. Chem. 40 (2002) 70–76.
[28] I.R. Gibson, W. Bonfield, Preparation and characterisation of magnesium/carbonate co-substituted hydroxyapatites, J. Mater. Sci. Mater. Med. 13 (2002) 685–693.
[29] I.R. Gibson, S.M. Best, W. Bonfield, Chemical characterisation of silicon-substituted hydroxyapatite, J. Biomed. Mater. Res. 44 (1999) 422–428.
[30] I.R. Gibson, Silicon containing apatites, in: P. Ducheyne, et al., (Eds.), Comprehensive Biomaterials, Elsevier Science, 2011, pp. 313–333, (ISBN: 978-0080553023).
[31] V.J. Mulley, C.D. Cavendish, A thermogravimetric method for the analysis of mixtures of brushite and monetite, Analyst 95 (1970) 304–307.
[32] N.W. Wikholm, R.A. Beebe, J.S. Kittelberger, Kinetics of the conversion of monetite to calcium pyrophosphate, J. Phys. Chem. 79 (1975) 853–856.
[33] G.R. Sivkumar, E.K. Girija, S. Narayana Kalkura, C. Subramanian, Crystallization and characterization of calcium phosphates: brushite and monetite, Cryst. Res. Technol. 33 (1998) 197–205.
[34] M. Yashima, Y. Kawaike, M. Tanaka, Determination of precise unit-cell parameters of the α-tricalcium phosphate Ca$_3$(PO$_4$)$_2$ through high-resolution synchrotron powder diffraction, J. Am. Ceram. Soc. 90 (2007) 272–274.
[35] M. Bohner, J. Lemaître, A.P. Legrand, J.D. De La Caillerie, P. Belgrand, Synthesis, X-ray diffraction and solid-state ^{31}P magic angle spinning NMR study of α-tricalcium orthophosphate, J. Mater. Sci. Mater. Med. 7 (1996) 457–463.
[36] R.J.B. Jakeman, A.K. Cheetham, N.J. Clayden, C.M. Dobson, A magic angle spinning NMR study of the phase diagram Ca$_{3-x}$Zn$_x$(PO$_4$), J. Solid State Chem. 78 (1989) 23–34.
[37] K.S. Tenhuisen, P.W. Brown, Phase evolution during the formation of α-tricalcium phosphate, J. Am. Ceram. Soc. 82 (1999) 2813–2818.